

Radiation re-solution of fission gas in non-oxide nuclear fuel

The Faculty of Oregon State University has made this article openly available.
Please share how this access benefits you. Your story matters.

Citation	Matthews, C., Schwen, D., & Klein, A. C. (2015). Radiation re-solution of fission gas in non-oxide nuclear fuel. <i>Journal of Nuclear Materials</i> , 457, 273-278. doi:10.1016/j.jnucmat.2014.11.108
DOI	10.1016/j.jnucmat.2014.11.108
Publisher	Elsevier
Version	Accepted Manuscript
Terms of Use	http://cdss.library.oregonstate.edu/sa-termsfuse

Radiation re-resolution of fission gas in non-oxide nuclear fuel

Christopher Matthews^{a,*}, Daniel Schwen^b, Andrew C. Klein^a

^a*Oregon State University, Nuclear Engineering and Radiation Health Physics, 3451 SW Jefferson Way, Corvallis OR*

^b*Fuel Modeling and Simulation, Idaho National Laboratory, P.O. Box 1625, Idaho Falls, ID 83415-3840, United States*

Abstract

Renewed interest in fast nuclear reactors is creating a need for better understanding of fission gas bubble behavior in non-oxide fuels. Collisions between fission fragments and their subsequent cascades can knock fission gas atoms out of bubbles and back into the fuel lattice, resulting in a loss term for the bubble. By assuming these collisions can be treated as binary collisions, we calculated a re-resolution parameter as a function of bubble radius. The calculations showed that there is a sharp decrease as bubble size increases until about 100 nm when the re-resolution parameter stays nearly constant. The bubble size dependence may explain the large bubble size distribution found in some uranium carbide and nitride fuels. Furthermore, our model shows ion cascades created in the fuel result in many more implanted fission gas atoms than collisions directly with fission fragments. Utilization of our calculated re-resolution parameter can be used to find a re-resolution rate for future bubble behavior simulations

1. Introduction

Recent investigations in fast reactor technology have focused on utilizing depleted uranium for in-situ conversion and utilization, with many designs hoping to employ a 30 year fuel pin lifetime [? ?]. For such long fuel lifetimes, the

*Corresponding author

Email address: `matthchr@engr.orst.edu` (Christopher Matthews)

5 highly energetic fission events will result in a nearly unrecognizable fuel form,
both physically and chemically. One in four fissions result in the production of
at least one volatile fission product that will tend to diffuse through the fuel
matrix, eventually collecting along the grain-boundaries. As burnup increases,
the individual bubbles along the grain boundaries will eventually interconnect to
10 form a network of inter-granular bubbles. Once these bubbles reach an outside
fuel surface, they will expel their contents into the fuel plenum. To extend fuel
lifetime, some sort fuel pin gas removal or venting will be necessary to prevent
cladding over-pressurization. In addition, many of the volatile fission products
are radioactive and must be carefully handled to prevent an uncontrolled envi-
15 ronmental release.

As fission gas atoms diffuse through the fuel, they can collect before they
reach the grain boundary and form stationary intra-granular bubbles, thus act-
ing as sinks for other passing gas atoms [?]. Fission fragments constantly
streaming through the fuel can knock atoms out of the bubbles, resulting in a
20 bubble loss term. Exactly how this process occurs has been described as either
a collisional atom-by-atom loss or by a complete destruction process. The lat-
ter theory assumes a bubble is destroyed and its gas atoms returned as single
atoms implanted into the fuel lattice if the bubble lies within a destruction zone
enclosed by a nanometer diameter cylinder around a given fission track. This
25 theory has seen success in oxide fuels [? ?], where the low electronic contribu-
tion to thermal conductivity of UO_2 results in a strong mechanical shockwave
surrounding the traveling fission fragment [?]. Furthermore while this model
can be applied to the small nanometer-sized bubble radii present in UO_2 fuels
[?], the model does not account for fission gas bubbles larger than the radius of
30 influence such as the hundred nanometer sized bubbles that have been observed
in non-oxide fuels [? ? ?]. A second microscopic theory first developed by
Nelson [?] assumes that individual gas atoms are knocked out of bubbles by the
cascades produced by fission fragments. In non-oxide ceramics such as uranium
carbide and nitride fuels, the energy transferred by a passing fission fragment is
35 more easily dissipated due to an overall higher thermal conductivity. As such,

the atomic collisions represented by Nelson's theory tends to underestimate re-resolution in oxide fuels, but represents the behavior of re-resolution in non-oxide fuels [?].

In order to successfully contain the fission gas, accurate models of single gas
40 atom and bubble behavior that can be used in full pin calculations are necessary
to estimate the mass and heat loading on a venting or cleanup system. Since the
ability of inter-granular bubbles to grow is dependent on the rate at which single
atoms reach the grain boundary, knowledge of the concentration of single gas
atoms in the fuel is necessary to calculate the size and interconnectivity of the
45 inter-granular bubbles. Intra-granular bubbles act as sinks for single gas atoms
thus estimation of their size and concentration distributions are necessary to
calculate the amount of free gas atoms available for diffusion. The equilibrium
size of the intra-granular bubbles will be a balance of growth due to temperature
dependent single atom absorption and loss due fission rate dependent knock out
50 process. In addition, the size of a given bubble will change both the source and
loss terms.

The focus of the current work is to develop a radius dependent re-resolution
parameter for use in fission gas bubble simulations. We have modified the Binary
Collision Approximation (BCA) code 3DTrim [?] to model fission gas bubbles
55 of different radii in a fission environment. By tracking the ion cascades produced
by fission fragments, we were able to track the fraction of atoms that escape
the bubble and become implanted in the surrounding fuel, resulting in a re-
solution parameter that can be used to calculate the total re-resolution rate. We
will show that the re-resolution parameter decreases drastically as radius increases
60 up to a threshold bubble radius. In addition we will show that direct fission
fragment collisions contribute much less to the total number of implanted fission
gas atoms than previously calculated. As a result, cascades created in the fuel
near the bubble surface play a much greater role in gas atom re-resolution.

2. Methodology

65 In his original 1969 formulation, Nelson estimated the re-solution rate of a
5 nm xenon gas bubble in UO_2 by assuming Rutherford potentials for fission
fragment collisions and a hard-sphere potential for all other collisions, with no
electronic losses. An atom was assumed to be implanted back into the fuel if
a gas atom located within a critical distance of 1 nm from the surface of the
70 bubble was struck by an ion and transferred a minimum energy $E_{min} = 300$
MeV [?]. Ronchi and Elton extended the calculation by allowing E_{min} , as well
as the radius of the bubble to be a variable parameter of the calculation in oxide
and carbide fuels.

In a more recent study, 3DTrim was utilized to determine the fission frag-
75 ment/fission gas collision frequency, while molecular dynamic simulations were
utilized to determine the probability of an atom being implanted using represen-
tative energies and depths [?]. The work here will extend the previous 3DTrim
simulations to non-oxide fuels and larger bubble radii, however the molecular
dynamic simulations will not be duplicated. Instead, 3DTrim will be directly
80 utilized to calculate the number of escaping fission gas atoms.

The code 3DTrim has been specially modified to model interactions with a
single bubble. 3DTrim utilizes the previously published TRIM algorithm [?] to
track ion cascades in non-Cartesian geometry. The TRIM algorithm utilizes the
Ziegler-Biersack-Littmark universal potential to model the interactions between
85 moving ions and stationary samples. Electronic losses are also considered and
vary based on the energy of the traveling ion. The ability of TRIM to quickly
analyze ion trajectories lies in the basic BCA simplification in which each colli-
sion is modeled as a single two-body collision. Although this approximation is
physically appropriate for high ion energies (typically above 1 keV), multi-body
90 collisions tend to occur at lower ion energies. While the inability of BCA to
treat multi-body collisions does not affect the dynamics of the highly energetic
fission fragment except at the end of their lives, the generated recoils can have
energies from 10 eV to 1 MeV. A second limitation is that channeling effects

are not taken into account in the traditional TRIM implementation, possibly
95 causing shortened ion paths through crystalline solids. In actuality, the 1 keV
limit may be higher than necessary in defining the applicability of BCA soft-
ware, and the channeling behavior may not be as drastic as previously thought
[? ?]. Although it is clear that the physical applicability of BCA erodes below
1 keV, the computational cost advantage of TRIM outweighs the limitations for
100 this study.

The simulation model consists of a 90% dense fuel cube with an implanted
sphere of xenon, krypton, and cesium gas, with concentrations based on average
fission fragment yield ratios (51%, 6%, and 43% respectively) [?]. At the
start of a 3DTrim simulation, two fission fragments are created based on the
105 probability distribution functions of typical fission fragment mass and energies.
These spawned ions are then inserted at a random location within the fuel and
assigned random, but opposite directions, and placed in a first in, first out ion
queue. 3DTrim then takes the first ion at the front of the queue and propagates
it through the material. As these ions progress, they will lose energy due to
110 electronic losses and will knock into other lattice or gas atoms, spawning new
recoils that are placed in the ion queue. The ions are killed once they drop
below a threshold energy of 5 eV. After appropriate calculations are completed,
the 3DTrim simulation picks the next ion at the front of the queue, propagates
it through the material and spawns new ions along the way. The simulation
115 continues until all ions in the list are propagated. In this way, all cascades are
followed until the atoms drop below the threshold energy. Due to the nature
of TRIM calculations, each ion interacts with an undamaged, 0 K amorphous
target.

A fission gas atom is considered implanted if it leaves the bubble surface
120 with a so-called implantation energy of 300 eV. Although Nelson's first proposed
the 300 eV limit as a threshold transfer energy E_{min} , more recent calculations
have found success using the 300 eV limit interchangeably as an implantation
energy limit [? ?]. By using an implantation energy limit as opposed to an
implantation distance limit, the BCA over-simplification at very low energies

125 can be avoided.

The total re-resolution rate at which atoms are knocked back into the fuel is:

$$\eta [\text{atom}/(\text{s} \cdot \text{m}^3)] = \int \dot{F} b(r) m(r) \rho(r) dr, \quad (1)$$

where r is the bubble radius, \dot{F} is the fission rate, b is the re-resolution parameter, m is the number of atoms in a bubble, and ρ is the bubble concentration distribution function:

$$N [\text{bub}/\text{m}^3] = \int \rho(r) dr. \quad (2)$$

130 Here, N is the total concentration of bubbles in the sample. Due to the large ranges of radii present in non-oxide fuels, the atomic density of the gas in the fuel was calculated using the van der Waals equation. In stress free solids, the number of atoms in a bubble m can be calculated as,

$$m = \frac{4}{3} \pi r^3 \left(B + \frac{2\gamma}{kTr} \right)^{-1} \quad (3)$$

135 where $\gamma = 1 \text{ N/m}$ is the surface energy of the material, k is Boltmanns constant, T is temperature, and $B = 8.5 \times 10^{-29} \text{ m}^3/\text{atom}$ [?].

Since the gas density in the bubble is always less that of the fuel, the model averaged density decreases as the total porosity model increases. The mean free path of an ion is inversely proportional to the density, thus a model with a lower average density will result in ions with an artificially increased lifetime. While 140 the travel length of most ions is too small for this to make a difference, the total path length of the fission fragments is on the order of micrometers, thus the lifetime and the number of produced cascades artificially increases as a function of porosity. This behavior leads to a slight increase in b that is dependent on the porosity of the model. By assuming the re-resolution rate is linearly dependent on 145 the path length, a correction factor can be applied to the re-resolution parameter to remove model size dependence:

$$b' = b \frac{\lambda_{fuel}}{\lambda_{fuel+bubble}} \quad (4)$$

where λ_{fuel} and $\lambda_{fuel+bubbles}$ are the average fission fragment path lengths in a pure fuel sample or fuel and bubble sample. In this way, simulations of various porosities can be normalized to a single re-resolution parameter line.

150 **3. Results**

Over 10^6 total fission events were modeled for a variety of radius and box size combinations. For each fission event, the number of implanted ions was counted, along with its original radial location within the bubble R_i , the implantation energy E_{min} , and implantation distance d . An ion was assumed implanted
 155 if it had an implantation energy greater than 300 eV. Since the error of the total implanted atom count goes by the square root, the number of fissions was increased until at least 10^6 implanted ions were counted so as to reduce the relative error to less than 0.1%.

Figure 1 displays the cumulative probability distribution of the ratio of R_i to
 160 bubble radius r in uranium carbide fuel. As expected, the majority of implanted atoms originate close to the surface of the bubble where there are fewer gas atoms with which to have a large-angle collision before exiting the bubble. Using the point at which the cumulative probability equals 0.5, a cross-over radii ratio C_r was determined at which equal numbers of escaped atoms come from larger or
 165 smaller radii. Although C_r does not vary drastically it reaches a threshold at very large radii, signifying that 50% of the escaped atoms originate in the outer eighth of the bubble.

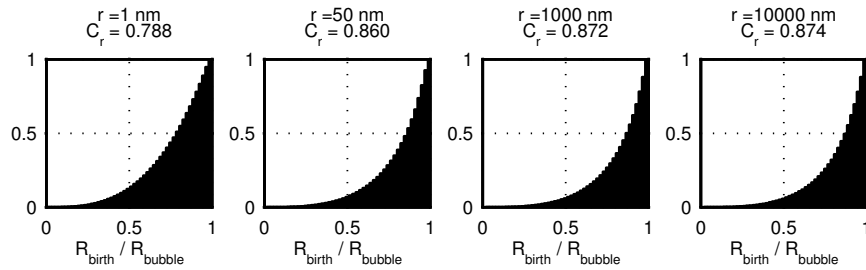


Figure 1: Cumulative probability distributions of the originating location of escaped fission gas atoms. The critical distance C_r is the ratio of the distance at which equal numbers of escaped fission gas atoms originated above and below the given bubble radius.

By cubing the ratio R_i/r , a cumulative probability distribution was created of the originating volume as seen in Figure 2. At small radii, the cumulative

170 probability is linear, signifying that all atoms in the bubble are equally available for re-resolution. However at large radii, the distribution bends slightly towards the outer volumes, signifying a lower probability of atoms originating from the center of the bubble.

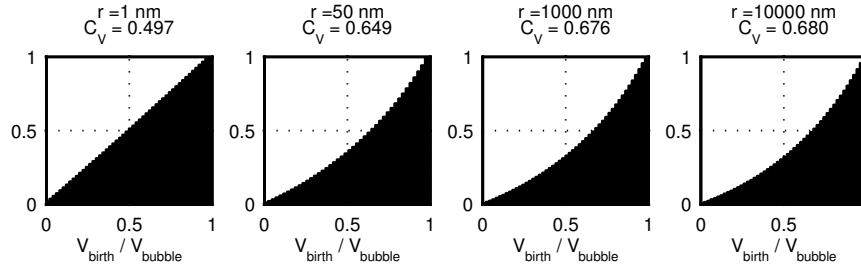


Figure 2: Cumulative probability distributions of the originating volume of escaped fission gas atoms. The critical distance C_V is the ratio of the distance at which equal numbers of escaped fission gas atoms originated above and below the given bubble volume.

Figure 3 displays the histogram data for implantation distances of the es-
 175 caped atoms. The plots are remarkably similar for all radii. Although there is a slight probability increase in large implantation distances for large bubbles, the vast majority of the escaped atoms come to rest very near the edge of the bubble.

As ions propagate through the material, they produce ions by knocking
 180 atoms from the lattice through a so-called parent-daughter interaction. In this way, each ion is a descendent of several different atoms, starting with a fission fragment ion. Figure 4 displays some of statistics associated with the parents and descendent behavior. The circles represent the fraction of escaped ions that are a fuel descendent, or rather have a uranium or carbon atom somewhere
 185 in their family tree. The fact that nearly 80-90% of all escaped atoms are a result of some sort of fuel interaction signifies the overwhelming importance of cascades originating outside the bubble. The remaining lines display the fraction of implanted ions with a fission fragment, gas, uranium, or carbon atom parent. For nearly all bubble radii, the direct fission fragment interaction
 190 remains roughly 10% due to the low cross-section of small bubbles and low

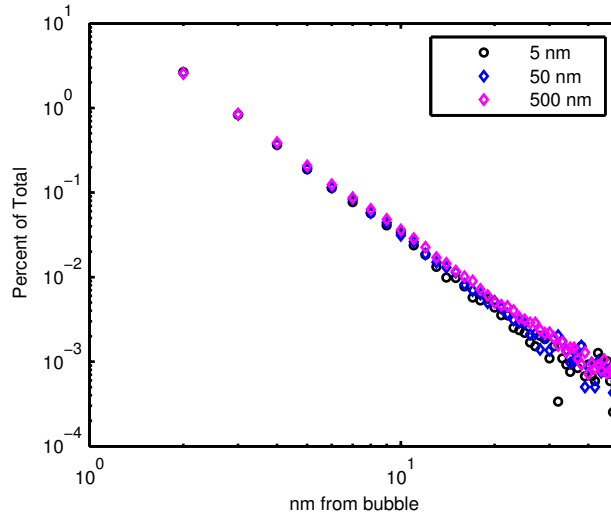


Figure 3: Histogram of implantation distances for various radii.

interaction probabilities for low density, large radii bubbles. For very small bubble sizes, nearly all collisions are a result of uranium atoms directly knocking out fission gas atom. As the radius increases, fission gas interactions with other fission gas atoms increase, becoming the most likely parent at bubble sizes greater than 5 nm. However, the relatively small decrease in fuel descendants
195 indicates that although gas parents are the most likely at large bubble radii, fuel cascades are still the root cause of an escaping atom. For all bubble radii, the relative importance of carbon atoms remains nearly insignificant.

As shown in Figure 4, the importance of fission fragment collisions is relatively minor compared with the importance of fuel interactions. However, it
200 can be expected that the highly energetic fission fragment will create daughter ions with relatively higher energies, thus resulting in more energetic and more deeply implanted atoms. This phenomenon can be shown by plotting the resolution rate as a function of E_{min} , displayed on the left side of Figure 5. For
205 low E_{min} energies, fuel cascades have a much higher importance in the total resolution rate than fission fragments, similar to what was displayed in Figure 4. However at a crossover energy of about 10 keV, fission fragment interactions

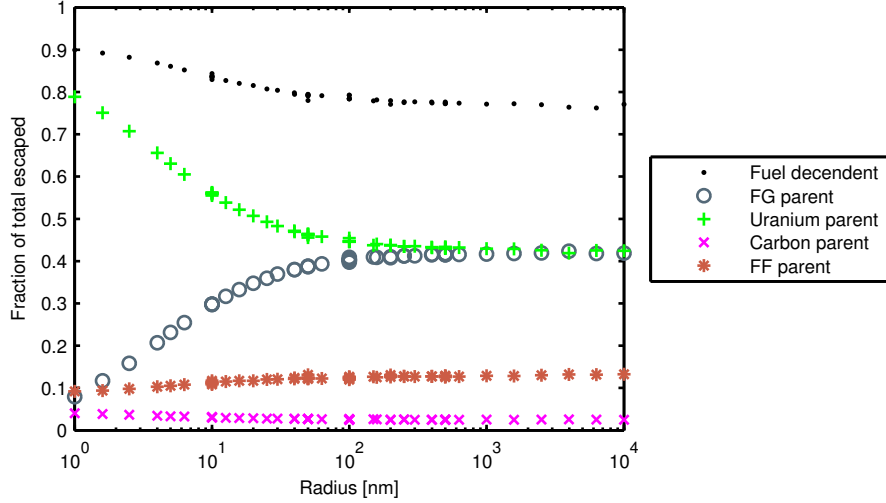


Figure 4: Fuel decendent and fission gas (FG), uranium, carbon, and fission fragment (FF) parent fractions as a function of bubble radius.

produce more implanted atoms than fuel cascades. Similar behavior occurs if a minimum distance from the bubble surface is utilized as the re-resolution criteria, as plotted on the right side of Figure 5. As to be expected, fission fragment interactions produce implanted ions that come to rest further away from the bubble edge than fuel interactions.

Figure 6 shows the re-resolution parameter b' as a function of radius. Initially, a sharp decrease in b' as radius increases occurs as the number of atoms in the bubble available for re-resolution decreases. However, as the bubble increases in size, the atomic density of the gas decreases, resulting in a larger mean free path of knocked gas atoms. This serves to slow the rapid decrease in the re-resolution parameter, resulting in a flattening for bubble radii larger than 100 nm. Also included is the uncorrected re-resolution parameter b for several simulations with the same cube size but with different bubble radii. At small bubble porosity, b lies on the corrected re-resolution parameter line. However as the bubble diameter approaches size of the model box, b increases, as would be expected with an artificially lengthened lifetime. The re-resolution parameter normalizes the

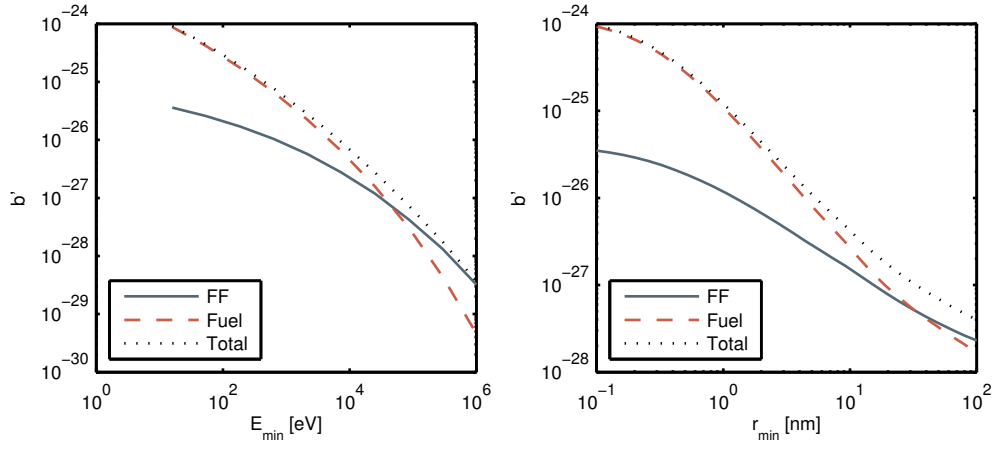


Figure 5: Re-resolution in a 5 nm bubble due to fission fragment and fuel cascades as a function of E_{min} and r_{min} .

artificially increased path lengths at large porosities, thus resulting in a single
 225 line for b for various combinations of radius and box size.

Finally, Figure 7 shows the corrected re-resolution parameter for uranium
 carbide, nitride and metal fuels. The three fuel-types have similar re-resolution
 parameters, with b' for uranium metal nearly double the other fuel types. Since
 the details of the collision in the TRIM algorithm mainly depend on the target
 230 type and density, the differences between nitride and carbide fuel are minimal
 since their densities are very similar and the atomic number of their non-metal
 atom differs by only one. The absence of any non-metal atom in the uranium
 metal fuel further enhances re-resolution due to all fuel interactions only occurring
 with the heavy uranium atom.

235 4. Discussion and Conclusions

For a bubble radius of 5 nm, we found the re-resolution parameter to be
 $1.4 \cdot 10^{-25}$ atoms/(s · m³), an order of magnitude less than previously calculated
 [? ?]. This smaller result is most likely due to the consideration of electronic
 energy losses for the ions, which were ignored in previous studies. By not

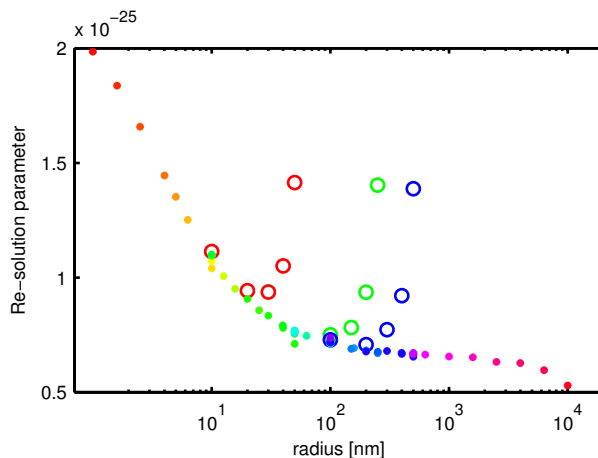


Figure 6: Calculated re-resolution parameter for uranium carbide for various radii and cube sizes. The circles corresponds to the uncorrected re-resolution parameter b for cube sizes 100 nm, 500 nm, and 1000 nm, while the dots display how the corrected re-resolution parameter b' falls along the same general line for all box sizes and radii.

240 accounting for electronic losses of traveling ions, the calculated path length of a given ion would be higher, resulting in a higher re-resolution rate.

From post previous irradiation examinations, the intra-granular bubbles in carbide and nitride fuel can be subdivided into two distinct groups: small P_1 bubbles with radius 1-30 nm and P_2 bubbles with radii ranging from 30-400 nm
 245 [?]. P_1 bubbles are present in nearly all irradiated samples, while the large P_2 bubbles occur in the hotter interior regions of the fuel pin. At low temperatures around the exterior of the fuel pin, slow gas atom diffusion leads to suppressed bubble growth and a lack of P_2 bubbles. As temperature increases the bubble source term also increases, resulting in larger bubbles. The re-resolution parameter decreases by a factor of 10 as the bubble radius changes from 1 nm to 100 nm
 250 signifying that larger bubbles are more stable than smaller bubbles, thus driving the bubble distribution to larger sizes. However for bubbles larger than 100 nm, the re-resolution parameter is relatively constant. This stabilization may explain the saturation bubble size of about 400 nm as seen experimentally; however
 255 further bubble population simulations are necessary to clarify the mechanics of

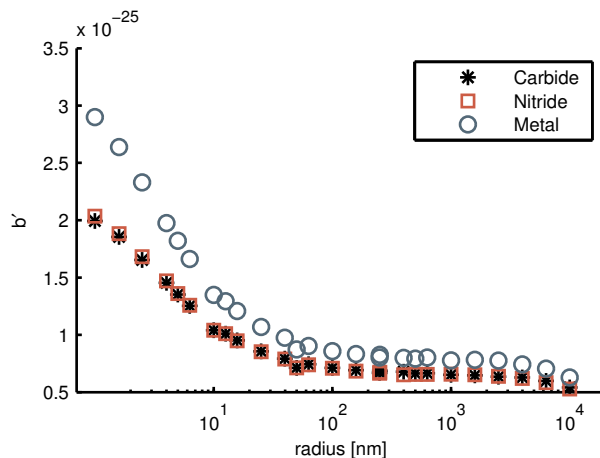


Figure 7: Re-resolution parameter for uranium carbide, nitride, and metal fuels.

such behavior.

One of the most interesting results from Ronchi and Eltons study was the increase in the re-resolution parameter at very large bubble sizes, especially as the minimum implantation energy increased [?]. This behavior was due to the very low atomic density in large bubbles, essentially allowing any knocked gas atom to escape the bubble. The re-resolution parameter calculated here does not exhibit that behavior in the range of the bubble sizes of interest (although at very large bubble sizes around 100 μm , a similar upward trend occurs). The difference can be attributed to the lower importance of fission fragment/fission gas interactions in the 3DTrim simulations. In Figure 4 the crossover to fuel/fission gas interaction importance occurs at implantation energies greater than 10^5 eV, while Elton and Ronchi calculated the crossover around 10^3 eV. Since the highly energetic fission fragments have the potential of producing more energetic recoils, increasing E_{min} selectively increases the importance of fission fragment collisions. Although the large bubbles do exhibit slightly more energetic escaped fission gas atoms, as visible in Figure 3, the increase is too slight to have an effect on the total the re-resolution parameter.

In conclusion, by assuming that fission gas re-resolution can be treated as

binary atomic collisions, we found a re-resolution parameter that was an order
275 of magnitude lower than previous studies, most likely due to the inclusion of
electronic ion energy losses. A sharp decrease in the re-resolution parameter as a
function of radius occurs, with a nearly constant re-resolution parameter after the
bubble reaches 100 nm. While the BCA approximation allowed the computa-
tionally cheap analysis of many different types of bubbles, the limitations at low
280 energies may skew the result, and further investigation into how valid the BCA
approximation for nuclear fuels is necessary. Regardless, similar trends in the
re-resolution parameter can be expected. The re-resolution parameter calculated
here can be used in rate-equation type simulations to model fission gas bubble
behavior, and ultimately fission gas release.

285 **Acknowledgements**

This research is being performed using funding received from the DOE Office
of Nuclear Energy's Nuclear Energy University Programs.

References